Strong dynamics, minimal flavor and R_b

Hidenori S. Fukano and Kimmo Tuominen
Department of Physics, University of Jyväskylä, P.O.Box 35, FIN-40014 Jyväskylä, Finland and Helsinki Institute of Physics, P.O.Box 64, FIN-00014 University of Helsinki, Finland

We show how models of electroweak symmetry breaking based on strong dynamics lead to observable contributions to the Z-boson decay width to $b\bar{b}$ pairs even in the absence of any extended sector responsible for dynamical generation of the masses of the Standard Model matter fields. These contributions are due to composite vector mesons mixing with the Standard Model electroweak gauge fields. Since such vectors are generally present in any model of dynamical electroweak symmetry breaking, our results lead to new stringent constraints on models of this type.

PACS numbers:

arXiv:1110.5248v1 [hep-ph] 24 Oct 2011

The Standard Model (SM) of elementary particle interactions is believed to be an incomplete theory due to its inability to explain the origin of the observed mass patterns of the matter fields, the number of matter generations and why there is excess of matter over antimatter. One possible paradigm beyond the Standard Model (BSM) is to apply strong coupling gauge theory dynamics. In Technicolor (TC) [1] , the electroweak symmetry breaking is due to the condensation of new matter fields, the technifermions. The vintage TC model based on the QCD-like gauge theory dynamics is incompatible with the electroweak precision data from the LEP experiments [2], and most of the modern model building within the Technicolor paradigm concentrates on the so called walking Technicolor (WTC) [3]. Here the Technicolor coupling constant evolves very slowly due to a nontrivial quasi stable infrared fixed point [4]. Models of WTC with minimal new particle content can be constructed by considering technifermions to transform under higher representations of the TC gauge group [5]. Technicolor only explains the mass patterns in the gauge sector of the SM via strong dynamics at the electroweak scale $\Lambda_{\rm TC} \simeq 1$ TeV. To explain various mass patterns of the known matter fields within a TC framework, further dynamical mechanism are needed; a well known example is the extended TC (ETC) [6]. An alternative to ETC, aimed to explain the large top quark mass and, in particular, the top-bottom mass splitting is the topcolor model and topcolor assisted technicolor model (TC2) [7].

One of the main experimental constraints on TC/ETC, and also on TC2, arises from the Z boson decay rate to $b\bar{b}$ pairs, more precisely one considers $R_b \equiv \Gamma(Z \to \bar{b}b)/\Gamma(Z \to {\rm had})$ [8, 9]. The importance of various contributions to this observable is determined by the relevant energy scale associated with different stages of the underlying dynamics: The effects from ETC gauge bosons are suppressed by the ETC scale $\Lambda_{\rm ETC} \gg \Lambda_{\rm TC}$, and similarly for the effects of the extended gauge interactions due to the topcolor dynamics. However, the effects from extra goldstone bosons due to topcolor, so called top-pions, are governed by the electroweak scale rather than the topcolor scale. It has been shown that their effect generally is a substantial reduction of R_b relative to the SM prediction and hence this provides stringent constraints on topcolor dynamics [9].

In this letter we point out an important refinement to this analysis. Namely, any TC model is already sensitive and subject for similar constraints *without any extension towards the matter sectors of SM*. This is so, since any TC model features composite vector and axial vector states in the spectrum which will mix with the SM gauge fields. We will explicate this issue within a generic low energy effective theory corresponding to the symmetry breaking pattern ${\rm SU}(2)_L \times {\rm SU}(2)_R \to {\rm SU}(2)_V$.

The experimental value of R_b [10] is

$$R_b^{\rm exp} \equiv \frac{\Gamma(Z \to \bar{b}b)}{\Gamma(Z \to {\rm had})} = 0.21629 \pm 0.00066. \tag{1}$$

It is convenient to divide $R_b = R_b^{\rm SM} + \Delta R_b$, where $R_b^{\rm SM}$ is predicted by the electroweak fit as [10]

$$R_b^{\rm SM} = 0.21578^{+0.00005}_{-0.00008}\,. \tag{2}$$

The quantity ΔR_b then encapsulates the contribution from the new physics (NP), and is represented as

$$\Delta R_b = 2R_b^{\rm SM}(1-R_b^{\rm SM}){\rm Re}\left[\frac{g_L^b\left[\delta g_L^b\right]_{\rm NP} + g_R^b\left[\delta g_R^b\right]_{\rm NP}}{(g_L^b)^2+(g_R^b)^2}\right]. \tag{3}$$

The experimental data constrains its value as

$$\Delta R_b = 0.00051 \pm 0.00066\,. \tag{4}$$

Eq.(3) is derived straightforwardly from [11] and $g_{L,R}^b$ is the SM tree level value given by

$$g_L^b = -\frac{1}{2} + \frac{1}{3}s_W^2\,, \quad g_R^b = \frac{1}{3}s_W^2\,, \tag{5}$$

The NP contribution $\left[\delta g_{L,R}^b\right]_{\rm NP}$ is

$$\begin{aligned}\left[\delta g_{L,R}^b\right]_{\rm NP} &= \left(\left[g_{L,R}^b\right]_{\rm BSM}^{\rm tree} - g_{L,R}^b\right)\\ &+ \left(\left[\delta g_{L,R}^b\right]_{\rm BSM}^{\rm 1\,loop} - \left[\delta g_{L,R}^b\right]_{\rm SM}^{\rm 1\,loop}\right). \end{aligned}\tag{6}$$

Given the model Lagrangian, one can therefore evaluate the tree level and one loop contributions and obtain a constraint on the model. The one loop contributions in $\left[\delta g^b_{L,R}\right]_{\rm NP}$ are obtained by calculating the Feynman diagrams in Fig.1. As a low energy effective Lagrangian,

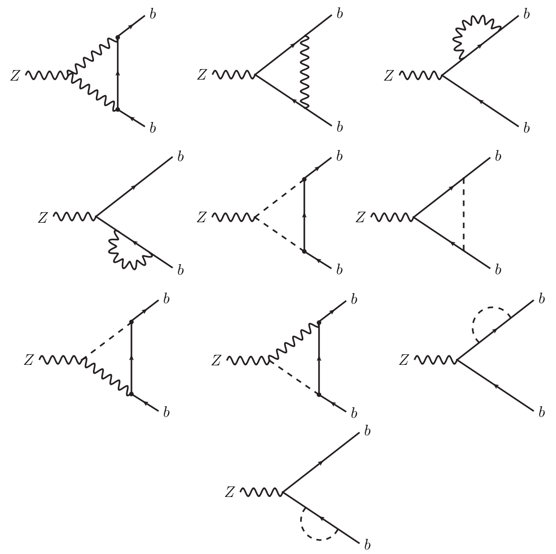

FIG. 1: The 1-loop Feynman diagrams for $\delta g^b_{L,R}$ in the Feynman gauge. The wave lines in the loops correspond to vector fields, while the dashed lines in the loops correspond to the would-be Golstone bosons. Only the top quark runs in the fermion loops.

we use a Lagrangian based on the generalized hidden local symmety (GHLS) [12]. This means that we consider the full symmetry group to be $G_{\rm glo}\times G_{\rm loc}$, where $G_{\rm glo}=SU(2)_L\times SU(2)_R$ and $G_{\rm loc}=SU(2)_L\times SU(2)_R$. The $G_{glo}\times G_{loc}$ breaks to the diagonal $[SU(2)_V]_{\rm glo}$. This symmetry breaking pattern features nine Nambu-Goldstone bosons (NGBs), which are the basic dynamical objects of the mode, and which we denote as $\tilde\pi^a$, $\tilde\pi^a_V$ and $\tilde\pi^a_A$ where $a=1,2,3$. The electroweak gauge group is embedded into the global symmetry $G_{\rm glo}$ in the usual manner, and its breaking leads to the masses of the electroweak gauge bosons via absorption of the would be NGBs $\tilde\pi^a$. Furthermore, the vector and axial-vector mesons, V^a_μ and A^a_μ, are included as dynamical gauge bosons of the hidden symmetry $G_{\rm loc}$, and their masses arise via absorption of six would-be NGBs, $\tilde\pi^a_V$ and $\tilde\pi^a_A$.

In Technicolor there is no direct coupling between the SM matter field and Technicolored matter or gauge fields. To understand how new physics contributions to the diagrams in Fig. 1 nevertheless arise, is simple: First, the only NGB field which can couple to the SM fermions is $\tilde\pi$, i.e. the field absorbed by the EW gauge bosons. This results in the following Yukawa coupling:

$$\mathcal{L}_{\Sigma\bar ff}=-\bar\psi_L\left[1+i\frac{\sqrt2\tilde\pi}{f_\pi}\right]\begin{pmatrix}m_t&0\\0&m_b\end{pmatrix}\psi_R+\text{h.c.}\,,\qquad(7)$$

where $\psi=(t,b)^T$ is $SU(2)$ doublet and $\psi_{L/R}\to g_{L/R}\psi_{L/R}$ under $G_{\rm glo}$. In this paper we consider only the third family quarks, and we set the $(3,3)$-component of the CKM matrix $V^{33}_{\rm CKM}$ equal to one. The contribution from $\mathcal{L}_{\Sigma\bar ff}$ can be removed by translating to the unitary gauge; for the numerical calculation we adapt the Feynman gauge.

Second, the SM fermions do not couple with the vector mesons V,A in the gauge eigenbasis:

$$\begin{aligned}\mathcal{L}_{\mathcal{G}\bar ff}&=e_0\tilde B_\mu\bar\psi\gamma^\mu\begin{pmatrix}2/3&0\\0&-1/3\end{pmatrix}\psi\qquad(8)\\&+\frac{e_0}{\sqrt2 s_\theta}\left[\tilde W^+_\mu\bar t\gamma^\mu\frac{1-\gamma_5}{2}b+\text{h.c.}\right]+\\&\frac{e_0}{c_\theta s_\theta}\tilde Z_\mu\bar\psi\gamma^\mu\left[g_L\frac{1-\gamma_5}{2}+g_R\frac{1+\gamma_5}{2}\right]\psi\,,\end{aligned}$$

where $\tilde B_\mu,\tilde W^\pm_\mu$ and $\tilde Z_\mu$ are SM gauge bosons in the gauge eigenbasis. The bare couplings in Eq.(8) are defined so that $e_0=gg'/\sqrt{g^2+g'^2}$ corresponds to the bare electric charge.

However, the propagating physical mass eigenstates, B_μ, $W^\pm_\mu$ and Z_μ for the vectors will be mixtures consisting of the states $\tilde W_\mu,\tilde B_\mu,\tilde V_\mu,\tilde A_\mu$. Similarly, the states $\tilde\pi,\tilde\pi_V,\tilde\pi_A$ will mix to provide for the propagating would-be NGB states. Due to these features, the interactions in Eqs. (7) and (8) are essentially different from the SM case. Consequentially, also the bare quantities arising in (8) are rescaled when we translate from gauge basis to the mass eigenbasis.

The detailed construction of the GHLS Lagrangian will be presented in detail in [15]. Here we will only describe some generic features of the analysis and present the numerical results.

The GHLS Lagrangian, free of any matter fields, $\mathcal{L}_0$, is given by

$$\mathcal{L}_0=\mathcal{L}_{\rm kin}+a\mathcal{L}_V+b\mathcal{L}_A+c\mathcal{L}_M+d\mathcal{L}_\pi\,,\qquad(9)$$

where a, b, c and d are dimensionless coefficients. The part $\mathcal{L}_{\rm kin}$ contains the usual kinetic terms for the electroweak gauge fields $\tilde W^a_\mu$ and $\tilde B_\mu$, and for the (composite) vector and axial-vector fields $\tilde V^a_\mu$ and $\tilde A^a_\mu$. We follow the analysis and notation of [12]. The coefficients a, b, c and d introduced above are unknown parameters which will be traded for dimensionfull parameters f^2_π, f^2_V and f^2_A related to the NGB fields and a dimensionless parameter χ. Hence, together with $\tilde g$, the self coupling of the vector and axial-vector fields, there are five parameters defining the model. Since the overall scale will be fixed with the electroweak scale, $v=246$ GeV, and the first Weinberg sum rule provides a nontrivial constraint among the decay constants, the number of free parameters will be reduced to three, which we will choose as $\tilde g$, M_A and χ.

Following [12], and expanding in the field fluctuations,

leads to a decomposition of $\mathcal{L}_0$ into

$$\mathcal{L}_0 = \mathcal{L}^{(2)}(\{\pi\},\{V\}) + \mathcal{L}^{(3)}(\{\pi\},\{V\}) + \cdots\,, \quad (10)$$

where $\{\pi\},\{V\}$ denote collectively $\{\tilde{\pi},\tilde{\pi}_V,\tilde{\pi}_A\}$ and $\{\tilde{W}_\mu,\tilde{B}_\mu,\tilde{V}_\mu,\tilde{A}_\mu\}$, respectively. The terms $\mathcal{L}^{(i)}$ in Eq.(10) each contain only terms with i fields, i.e. $\mathcal{L}^{(2)}$ are the quadratic terms, $\mathcal{L}^{(3)}$ trilinear terms, etc.

The full Lagrangian is given by

$$\mathcal{L} = \mathcal{L}_{\rm kin} + \mathcal{L}_{\rm mass} + \mathcal{L}^{(3)}(\{\pi\},\{V\}) + \mathcal{L}_{\Sigma\bar{f}f} + \mathcal{L}_{\mathcal{G}\bar{f}f}, \quad (11)$$

where $\mathcal{L}_{\rm kin}$ and $\mathcal{L}_{\rm mass}$ are the kinetic term and mass terms for would-be NGBs, vector bosons and quarks. The parts $\mathcal{L}_{\Sigma\bar{f}f}$ and $\mathcal{L}_{\mathcal{G}\bar{f}f}$ contains interactions of the SM fermions. From the quadratic part $\mathcal{L}^{(2)}$ we solve for the mass eigenstates, and the interactions arising from the trilinear part and from fermion interaction terms are then written in terms of the propagating mass eigenstates.

The electric charge eigenstates are defined in the usual manner: e.g. $W^\pm = (W^1_\mu \mp W^2_\mu)/\sqrt{2}$ and similarly for the other V, A states. After diagonalization of the mass matrices we find that the eigenvalues for the charged bosons are

$$\begin{aligned}
M_W^2 &= \frac{1}{2}g^2 f_\pi^2\left[1 - \frac{1+\chi^2}{2}\epsilon_0^2 + \mathcal{O}(\epsilon_0^4)\right]\,,\\
M_{V^\pm}^2 &= \tilde{g}^2 f_V^2\left[1 + \frac{1}{2}\epsilon_0^2 + \mathcal{O}(\epsilon_0^4)\right]\,,\\
M_{A^\pm}^2 &= \tilde{g}^2 f_A^2\left[1 + \frac{\chi^2}{2}\epsilon_0^2 + \mathcal{O}(\epsilon_0^4)\right]\,. \quad (12)
\end{aligned}$$

For the neutral bosons we have $M_B^2 = 0$ (massless photon) and

$$\begin{aligned}
M_Z^2 &= \frac{g^2 f_\pi^2}{2c_\theta^2}\left[1 - \frac{c_{2\theta}^2+\chi^2}{2c_\theta^2}\epsilon_0^2 + \mathcal{O}(\epsilon_0^4)\right]\,,\\
M_{V^0}^2 &= \tilde{g}^2 f_V^2\left[1 + \frac{1}{2c_\theta^2}\epsilon_0^2 + \mathcal{O}(\epsilon_0^4)\right]\,,\\
M_{A^0}^2 &= \tilde{g}^2 f_A^2\left[1 + \frac{\chi^2}{2c_\theta^2}\epsilon_0^2 + \mathcal{O}(\epsilon_0^4)\right]\,. \quad (13)
\end{aligned}$$

In the above equations $\tilde{g}$ is the self-coupling of the vector and axial vector fields and we have expanded in $\epsilon_0 \equiv g/\tilde{g}$. Since $\tilde{g}$ is a strong coupling of $\mathcal{O}(1\ldots 10)$ this is a small number. As we already mentioned, there are altogether five parameters in the effective Lagrangian, $\tilde{g}$, f_π, f_V, f_A and χ . These can be reduced down to three independent parameters as follows. First, to relate with existing literature, we note that χ in our model, is the same χ which appears in [13] and corresponds to $1-\chi$ in [14]. Next, in accordance with [13], note that the physical electroweak gauge couplings are given by $(g^2_{\rm EW})^{-1} = (g^2)^{-1}\left[1+(1+\chi^2)\epsilon_0^2/2\right]$ and $(g'^2_{\rm EW})^{-1} = (g'^2)^{-1}\left[1+(1+\chi^2)t_\theta^2\epsilon_0^2/2\right]$ and the Weinberg angle as $\tan\theta \equiv t_\theta = g'_{\rm EW}/g_{\rm EW}$. Note that $\epsilon_0 = g/\tilde{g}$ is equal to $\epsilon \equiv g_{\rm EW}/\tilde{g}$ up to $\mathcal{O}(\epsilon^4)$ corrections, and it is convenient to expand in ϵ instead of ϵ_0. The Weinberg sum rule is a statement relating the physical decay constants, $F_\pi^2 = F_V^2 - F_A^2$. The decay constants $F_{V,A}$ are defined by the residue at the pole of the two point vector and axial-vector current correlators. The decay constant of the physical techni-pion, F_π, is defined as

$$M_W^2 = \frac{1}{2}g^2 f_\pi^2\left[1 + \frac{1+\chi^2}{2}\epsilon^2 + \mathcal{O}(\epsilon^4)\right] \equiv \frac{1}{2}g_{\rm EW}^2 F_\pi^2\,, \quad (14)$$

and numerically $F_\pi^2 = 1/(2\sqrt{2}G_F) \simeq (174\,\mathrm{GeV})^2$, for $G_F = 1.16637\times 10^{-5}\,\mathrm{GeV}^{-2}$ [16]. Up to $\mathcal{O}(\epsilon^4)$, we have $F_\pi^2 = f_\pi^2$, and also $F_V^2 = f_V^2$ and $F_A^2 = \chi^2 f_A^2$. Therefore, up to $\mathcal{O}(\epsilon^4)$, the first Weinberg sum rule is represented as

$$f_V^2 = F_\pi^2 + \chi^2 f_A^2\,, \quad (15)$$

and we use this relation to express $M_{V^\pm}$ in Eq.(12) as a function of $\tilde{g}$,F_π, f_A. In addition, χ is related to the oblique S parameter via

$$S = \frac{8\pi(1-\chi^2)}{\tilde{g}^2}\,, \quad (16)$$

From the viewpoint of the effective model, S is a parameter whose value depends on the dynamics of the underlying strong dynamics. We do not wish to commit to any particular underlying theory sharing the same global symmetry breaking pattern as our effective model, and consider S as a free parameter with $\tilde{g}$ and M_A.

We now proceed to evaluate the contribution to ΔR_b and return to consider Eq.(6). At the tree level we have

$$\begin{aligned}
\left[g_L^b\right]^{\rm tree}_{\rm BSM} &= \left(-\frac{1}{2}+\frac{1}{3}s_\theta^2\right)v_Z^1 - \frac{1}{3}c_\theta s_\theta v_Z^0\,,\\
\left[g_R^b\right]^{\rm tree}_{\rm BSM} &= \frac{1}{3}s_\theta^2 v_Z^1 - \frac{1}{3}c_\theta s_\theta v_Z^0\,, \quad (17)
\end{aligned}$$

where $v_Z^0 = -c_{2\theta}\,t_\theta\epsilon^2$ and $v_Z^1 = 1-(c_{2\theta}^2+\chi^2)/(4c_\theta^2)\epsilon^2$, up to $\mathcal{O}(\epsilon^4)$. For the numerical computation of ΔR_b we use the *FeynRules* [17] and *FeynArts/FormCalc/LoopTool* [18] to implement the interactions from the effective Lagrangian Eq.(11). The calculation is performed in the Feynman gauge

First, we consider our model at the limit $\epsilon\to 0$ without the Weinberg sum rule. In this limit the model corresponds to SM, and we obtain following values for $\left[\delta g^b_{L,R}\right]^{\rm 1\,loop}_{\rm SM}$:

$$\mathrm{Re}\left[\delta g_L^b\right]^{\rm 1\,loop}_{\rm SM} = 0.00579\,,\quad \mathrm{Re}\left[\delta g_R^b\right]^{\rm 1\,loop}_{\rm SM} = 0\,, \quad (18)$$

for $\alpha^{-1}(M_Z) = 128.9$, $G_F = 1.16637\times 10^{-5}\,\mathrm{GeV}^{-2}$ and $m_t = 172.9\,\mathrm{GeV}$ [16] where α is the fine structure constant at the Z-pole. This result is consistent with the one loop results in e.g. [19], if we account for the change in

the value of m_t. Then, we obtain the NP contribution to ΔR_b numerically for the present model, Eq.(11). These numerical results for ΔR_b are shown in Figs. 2 and 3. The constraints from Eq.(16) and the first Weinberg sum rule, Eq.(15), are taken into account.

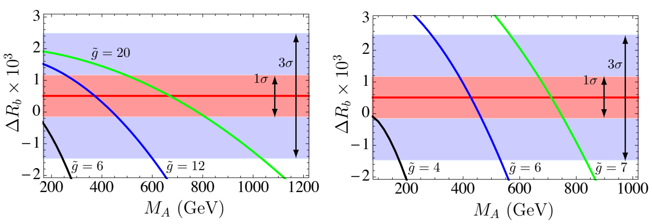

FIG. 2: ΔR_b as a function of M_A. The left panel is for $S = 0$ with $\tilde{g} = 6, 12, 20$ and the right panel is for $S = 0.3$ with $\tilde{g} = 4, 6, 7$. The shaded regions are 1σ (thinner horizontal band), and 3σ (thicker horizontal band) allowed regions from the constraint in Eq.(4).

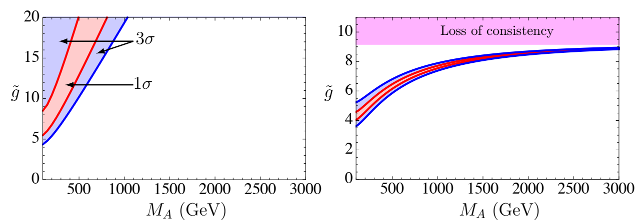

FIG. 3: The constraint on R_b in the $(M_A, \tilde{g})$-plane for $S = 0$ (left panel) and $S = 0.3$ (right panel). The thinner (thicker) shaded region corresponds to the 1σ (3σ) allowed region. The upper shaded region in the right panel shows the consistency of the model.

In Fig.2, we show ΔR_b as a function of M_A for several values of $\tilde{g}$ with $S = 0$ (left panel) and $S = 0.3$ (right panel). In Fig.3, we show the R_b constraint on $(M_A, \tilde{g})$-plane corresponding again to $S = 0$ and 0.3. From Fig.3 we observe that the region allowed by the R_b constraint is limited to a very narrow area on the $(M_A, \tilde{g})$-plane even if the flavor sector is introduced in the most minimal way. The upper shaded region in the right panel in Fig.3 corresponds to the bound $\chi^2 < 0$ which implies that $\tilde{g} < 8\pi/S$ from Eq.(16). In this region the theory itself loses consistency.

Under the present 3σ constraints for R_b, the axial vector meson with $M_A \simeq 600\,\text{GeV}$ for $\tilde{g} \simeq 7$ and $S = 0.3$ may be discovered at the LHC with 100 fb^{-1} at 13 TeV via the $pp \to A^\pm \to l\nu$ process if the leptons also couple to the GHLS sector as Eqs.(8) [20].

We have studied a generic effective Lagrangian for dynamical electroweak symmetry breaking and demonstrated that the R_b constraints are important even in the absence of extended dynamics required in this type of models for the generation of SM fermion masses. The global symmetry of our Lagrangian was taken to be $SU(2)_L \times SU(2)_R$ spontaneously breaking to $SU(2)_V$. A possible underlying model which would realize our results are Technicolor with SU(3) gauge group and two sextet fermions.; this theory has naive perturbative S parameter equal to 0.3. Our results show that large M_A is compatible with data only if S is sufficiently large, which will increase the tension with respect to the precision electroweak data. Moreover, since simple strong dynamics we have considered here, is likely in need to be enlarged to accommodate dynamical mechanisms for fermion mass generation, the constraints are likely to be even tighter: such new sources typically yield further negative contributions to R_b, and this may lead to further suppression of phenomenologically viable values of M_A.

Our study was carried out for the GHLS type nonlinear sigma model Lagrangian with a minimal coupling to SM flavors. Therefore, our results can be directly applied to several models sharing the same global symmetry at low energies.

[1] S. Weinberg, Phys. Rev. D **13**, 974 (1976); Phys. Rev. D **19**, 1277 (1979), L. Susskind, Phys. Rev. D **20**, 2619 (1979).

[2] M. E. Peskin, *et al.* Phys. Rev. Lett. **65**, 964-967 (1990); M. E. Peskin, *et al.* Phys. Rev. **D46**, 381-409 (1992).

[3] B. Holdom, Phys. Lett. B **150**, 301 (1985); K. Yamawaki *et al.* Phys. Rev. Lett. **56**, 1335 (1986); T. Akiba *et al.* Phys. Lett. B **169**, 432 (1986); T. W. Appelquist *et al.* Phys. Rev. Lett. **57**, 957 (1986).

[4] T. Banks and A. Zaks, Nucl. Phys. B **196**, 189 (1982).

[5] F. Sannino, K. Tuominen, Phys. Rev. **D71**, 051901 (2005); D. D. Dietrich, F. Sannino, K. Tuominen, Phys. Rev. **D72**, 055001 (2005).

[6] S. Dimopoulos *et al.* Nucl. Phys. B **155**, 237 (1979); E. Eichten *et al.* Phys. Lett. B **90**, 125 (1980).

[7] C. T. Hill, Phys. Lett. B **266**, 419 (1991); C. T. Hill, Phys. Lett. **B345**, 483-489 (1995); G. Buchalla *et al.* Phys. Rev. **D53**, 5185-5200 (1996).

[8] R. S. Chivukula *et al.* Phys. Lett. **B331**, 383-389 (1994).

[9] G. Burdman *et al.* Phys. Lett. **B403**, 101-107 (1997).

[10] M. Baak *et al.*, arXiv:1107.0975 [hep-ph].

[11] W. F. L. Hollik, Fortsch. Phys. **38**, 165-260 (1990).

[12] M. Bando, *et al.* Prog. Theor. Phys. **79**, 1140 (1988).

[13] A. Belyaev, *et al.* Phys. Rev. **D79**, 035006 (2009).

[14] R. Foadi, *et al.* Phys. Rev. **D76**, 055005 (2007).

[15] H. S. Fukano and K. Tuominen, in progress.

[16] KNakamura *et al.*, J. Phys. G **G37**, 075021 (2010).

[17] N. D. Christensen, C. Duhr, Comput. Phys. Commun. **180**, 1614-1641 (2009).

[18] T. Hahn, Comput. Phys. Commun. **140**, 418-431 (2001).

[19] P. Bamert, *et al.* Phys. Rev. **D54**, 4275-4300 (1996).

[20] J. R. Andersen, T. Hapola, F. Sannino, [arXiv:1105.1433 [hep-ph]].